3.06 Artificial Retinas

Wilfried Mokwa, Institute of Materials in Electrical Engineering 1, RWTH Aachen University, Aachen, Germany

Glossary

AIROF Anodic/Activated Iridium Oxide
CDC Charge Delivery Capacity
CMOS Complementary Metal Oxide Semiconductor
DSP Digital Signal Processor
FDA Food and Drug Administration
FES Functional Electrostimulation
MEMS Microelectromechanical Systems
RF-BPN Receptive Field–Adaptive Biology–Inspired Pulse Processing Neural Network
RF Radio Frequency
RP Retinitis Pigmentosa
SIROF Sputtered Iridium Oxide Film
USP United States Pharmacopeia

3.06.1 Introduction

The most frequent cause of blindness is the degeneration of retinal cells. In developed countries macula degeneration is the main cause of blindness and strong visual impairment. About 25–30 million people are suffering from this disease. During the course of this disease the tissue of the macula is first destroyed. This leads to a complete loss of vision in the center. Reading is no longer possible for these patients. Another group of people suffer from retinitis pigmentosa (RP), a genetic disorder. The worldwide number amounts to 1–3 million affected persons. This disease often starts with night blindness.

Contrast and color vision as well as visual acuity diminish. Peripheral vision diminishes first. The field of vision becomes narrower and is completely lost in later stages. These symptoms are because of the degeneration of the light-sensitive rods and cones of the retina. This process can continue for decades depending on the individual concerned. **Figure 1** shows a photograph of a normal and a degenerated retina.

Bypassing the nonworking retina or the optic nerve by a technical implant might restore some vision to these patients. Brindley and Lewin (1968) were the first who tried to develop a visual prosthesis that stimulates the visual cortex directly for blind people.

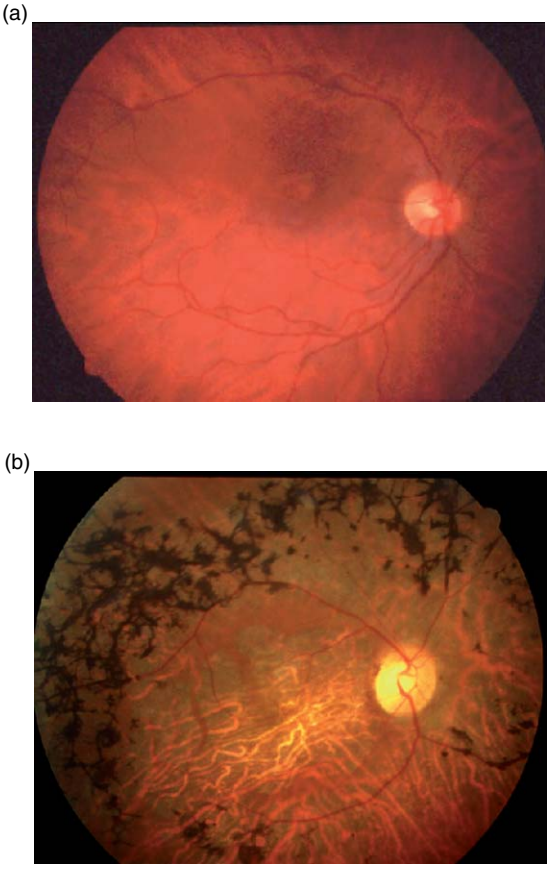

Figure 1 (a) Photograph of a normal human retina. The yellow spot in the right part is the optic disk where the optic nerve leaves the eye. It has a diameter of about 3 mm. (b) Photograph of a degenerated retina of a retinitis pigmentosa (RP) patient. The degenerated regions at the outer border look black. The field of vision is drastically reduced to the central part of the retina. (Courtesy P Walter, Department of Ophthalmology, University Hospital, RWTH Aachen University, Aachen, Germany.)

3.06.2 Physiology of the Human Eye

A cross section of the human eye is shown in **Figure 2** . The outer tissue consists of three different layers: the sclerotic coat, the choroidic coat, and the retina. The retina is the inner layer of the eye and contains the light receptors: the rods and the cones (**Figure 3**). The number of rods is about 60–125 million. Rods are extremely sensitive to light but do not provide a sharp image. They allow us to see in the dark and are responsible for peripheral vision. The number of cones is about 3–6.5 million. They need bright light to be functional. Cones are responsible for seeing colors and provide us with sharp images. An area with a diameter of about 5 mm around the central axis of the retina is called the macula, the region for sharp vision. In the center of the macula, there is a small pit with a diameter of about 1.5 mm, the fovea, the center responsible for sharpest vision. Here the cones are present at a very high density (10%). It is important to emphasize that the rods and cones are beneath a layer of neural cells. Light enters the eye through the cornea, the pupil, and the lens; passes the vitreous body and the neural cells; and is absorbed by the cones and rods. Here the light is converted into nerve pulses that are transferred via different neural cells (bipolar and ganglion cells) to the brain through the optic nerve. Within the visual cortex, a region of the brain that is responsible for visual perception, the incoming pulses are interpreted and converted to a picture. In the eyes of vertebrates, signal processing starts in the retina. There is a complex array of interneurons (amacrine and horizontal cells) that form synapses with the bipolar and ganglion cells by forming a neural network that modifies the activity (**Figure 3**). By this a preprocessing of the signals is achieved, leading, for example, to an increase in contrast. More detailed information on the physiology of the eye can be found in Kaufman and Alm (2003).

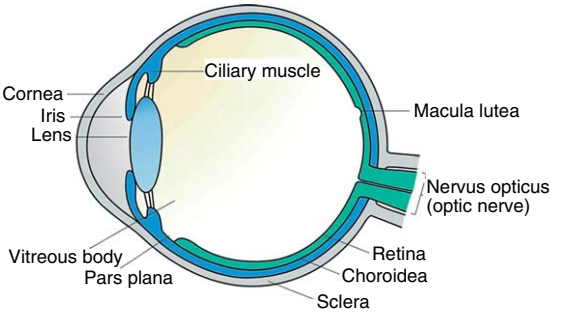

Figure 2 Schematic cross section of the human eye. (Courtesy IIP Technologies, Bonn, Germany.)

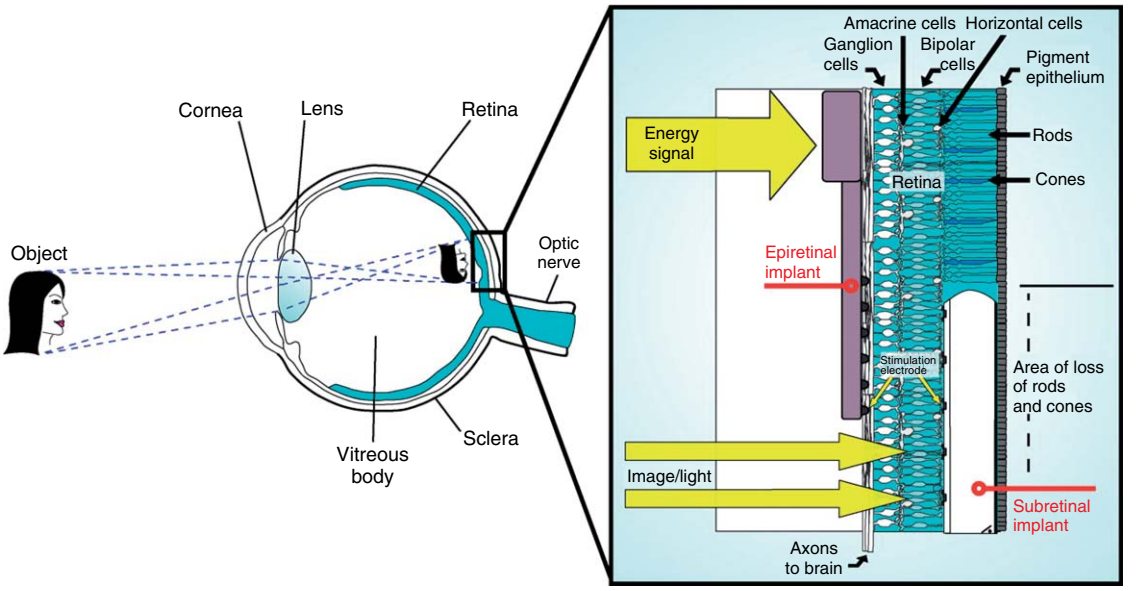

Figure 3 Cross section of the human eye illustrating the epiretinal and the subretinal approach. (Source: Reprinted with permission from Zrenner E 2002 Will retinal implants restore vision? *Science* **295**, 1022–5. Copyright 2002 AAAS.)

3.06.3 Possible Approaches to Restore Vision by Electrical Stimulation of Nerve Cells

3.06.3.1 Retinal Implants

3.06.3.1.1 System concept

Studies have found that about 30% of retinal ganglion cells of RP patients are still functional even after several years of blindness. It has been shown that electrical stimulation of ganglion cells inside the eye at the inner surface of the retina results in visual sensations (Benjamin *et al.* 1994, Santos *et al.* 1997, Stone *et al.* 1992). Therefore, bypassing the degenerated photoreceptors by electrically stimulating the retinal ganglion cells seems possible (Humayun *et al.* 1996, 1999, Walter Heimann 2000, Wyatt *et al.* 1994). By this, action potentials are evoked in retinal ganglion cells, causing a visual sensation.

Most approaches presented up to now for a retinal implant use, besides the implant, an extraocular part that records visual images. The images are transformed by a digital signal processor (DSP) into corresponding signals for stimulation of the nerve cells. These signals are transmitted to the receiver unit of an implant. Integrated circuitry of this unit decodes the signals and transfers the data to a stimulation circuitry that selects stimulation electrodes of the implant and generates current pulses to the electrodes (Schwarz *et al.* 2000). By this, action potentials in the nerve cells of the retina, in the optic nerve, or in the nerve cells of the visual cortex are evoked, causing a visual sensation.

3.06.3.1.2 Subretinal stimulation

Several groups are working on the concept of subretinal stimulation (e.g., Chow 1993, Peachey and Chow 1999, Sachs and Gabel 2004, Schwahn *et al.* 2001, Zrenner 2002, Zrenner *et al.* 1999).

In the subretinal approach the degenerated photoreceptors are replaced by a chip that has a microphotodiode array together with a stimulation electrode array implanted in it (**Figures 3** and **4**). By using the natural optics of the eye an image is mapped onto the photodiode array. The photodiodes respond to the incoming light. Depending on the output of the photodiodes, on-chip electronics generate the necessary stimulation currents that activate healthy bipolar and ganglion cell layers of the retina. Positioning and fixation of the implant are relatively easy. No external camera or image processing is needed. Eye movement can be used to localize objects. A basic requirement for this approach to work is that the optics of the eye should still be functional. Because of the necessary on-chip electronics, energy is required for operation and it has to be supplied externally by means of electromagnetic or optic coupling.

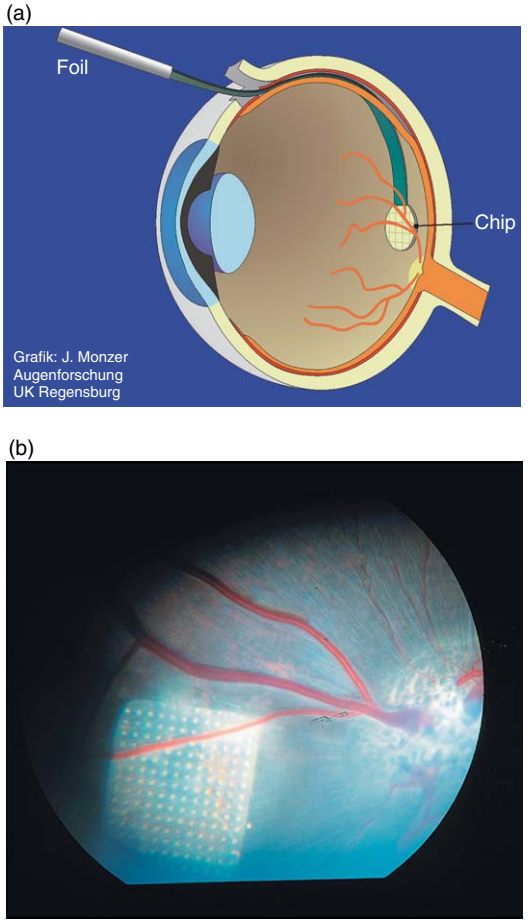

Figure 4 (a) Schematic view of the subretinal approach. (b) View of a subretinal implant through the ganglion cell layer. The implant has an area of 3 mm × 3 mm and a thickness of 50 μm. One thousand five hundred pixels are on this implant with a pixel size of 70 μm × 70 μm. It can be clearly seen from the blood vessel over the implant that the implant is located subretinally. (Courtesy Retinal Implant AG, Reutlingen, Germany.)

3.06.3.1.3 Epiretinal stimulation

In contrast to subretinal stimulation, in epiretinal implants the stimulation electrodes are placed on the inner side of the retina (compare **Figure 3**). Therefore, retinal ganglion cells are stimulated where some preprocessing of the signals has already taken place. This preprocessing has to be considered when transforming the visual information recorded by a camera into data stimulation patterns. Eckmiller (1995, 1996, 1997) was the first to introduce the concept of a retina encoder simulating the neural network of the retina.

The concept of an epiretinal system can be illustrated through **Figure 5** (Schwarz *et al.* 2000). The system consists of an extraocular and an intraocular part. The components of the extraocular part are a complementary metal oxide semiconductor (CMOS) image sensor for capturing visual images, an artificial neural net that imitates the functions of different ganglion layers of the retina (retina encoder), and a transmitter. The visual images are transformed by the neural net into control signals for the stimulation electrodes (Mokwa 2004). These signals are finally transmitted into the interior of the eye together with the energy needed to supply the intraocular part. For the energy transfer a radio frequency (RF) link is used (Mokwa 2004) and for data transfer an RF link (Mokwa 2004) or an optic link is used (Laube *et al.* 2004a). The intraocular part of the system consists of a receiver circuitry where energy and data signals are separated, the clock signal is extracted, and the data signals are decoded. These data are transferred via a microcable to the stimulation unit. An integrated circuitry decodes the information from the serial data stream. From this information the requested electrode is selected and current pulses are generated. **Figure 6** shows an encapsulated implant that was developed by the German EPIRET team and was successfully tested in animals (Laube *et al.* 2004a, b, Mokwa 2004, Walter *et al.* 2005).

Second Sight and partners introduced a similar system based on a cochlea implant (Humayun *et al.* 2003). The whole electronics are mounted on the outer side of the sclera. From there a cable is laid through the sclera into the eye. The cable connects a 4 × 4 stimulation electrode array that is fit into the retina (**Figure 7**).

3.06.3.2 Stimulation of the Optic Nerve

In the optic nerve about 1 million nerve fibers connect the retina with the visual cortex. It is possible to reach the optic nerve through surgery. The idea of realizing a visual prosthesis by stimulating the optic nerve was conceived by Thomas Mortimer and Claude Veraart in the early 1990s (Veraart *et al.* 1998). **Figure 8** shows a schematic view of the system.

For stimulation of the fibers a cuff electrode is wound around the optic nerve. This cuff is connected to implanted stimulation electronics. Information is exchanged with the implanted system via telemetry. The team of Claude Veraart developed a spiral cuff that was made from rubber and flexible silicone (**Figure 9**). The first version was equipped with four platinum contacts and a later version with eight. The electrode diameter is about 3 mm;

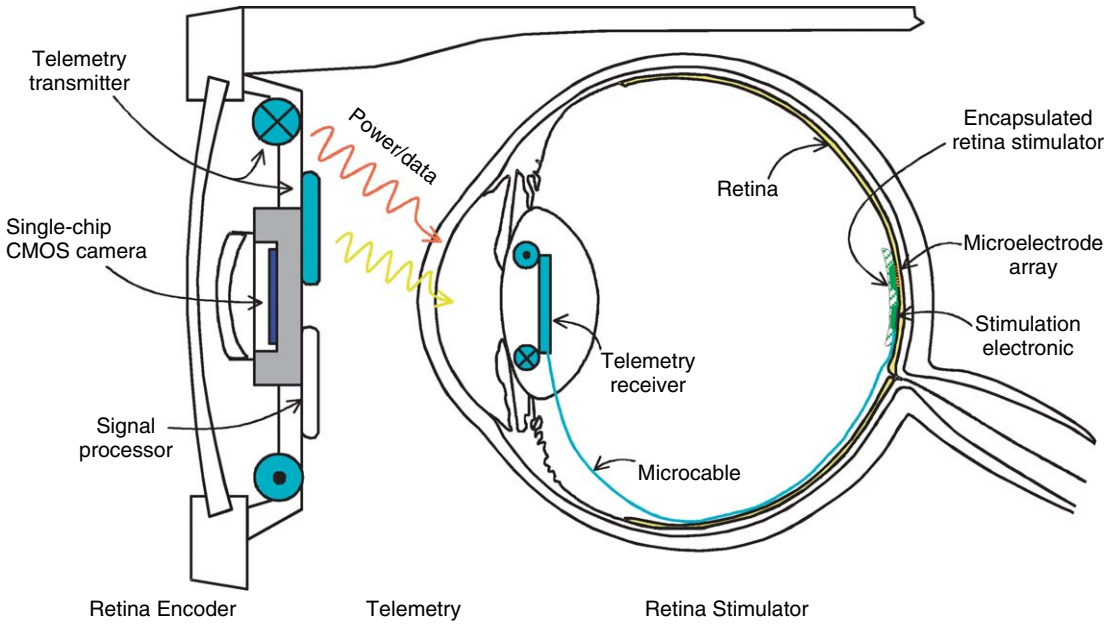

Figure 5 System concept of a visual prosthesis for epiretinal stimulation.

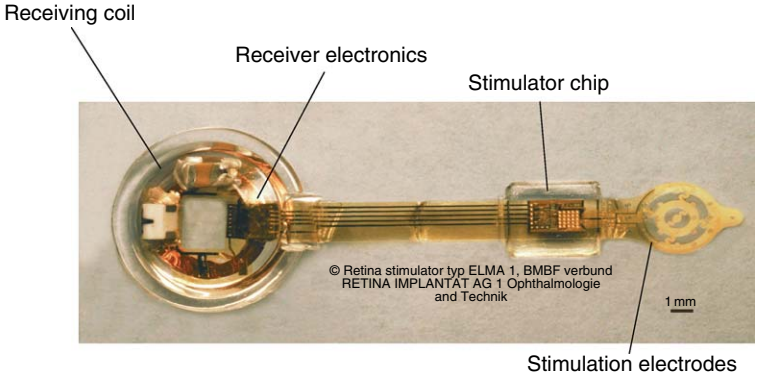

Figure 6 Photograph of an encapsulated retinal implant. The left part is formed like an artificial lens. This lens contains the receiver coil and the chip. A microcable connects the receiver electronics with the stimulator chip. At the right, the stimulating electrodes are visible. The whole implant is encapsulated with silicone.

stimulator dimensions are 25 mm× 30 mm with a 6-mm thickness. To avoid any lesion of the optic nerve the geometry of the cuff allows to adapt continuously to the diameter of the optic nerve while at the same time guaranteeing close contact between the electrode and the nerve. The first implantation of the system was performed in February 1998 by Prof. C. Raftopoulos of the Neurosurgery Unit, St-Luc's University Hospital, UCL, Brussels, on a long-term RP patient (Veraart *et al.* 1998). A spiral cuff was implanted intracranially around the right optic nerve. The cable of the cuff was connected to the implanted connector and was brought through the skin at the clavicle level where it ended in an external connector. By this, optic nerve stimulation could be achieved by using external stimulators. After a brief period of convalescence, the optic nerve fibers were electrically stimulated. The patient reported on sensations (phosphenes) generated by the stimulation of the optic nerve that were exclusively visual. These phosphenes can be obtained at low thresholds. The characteristics of the phosphenes depend on the conditions of electrical stimulation like pulse shape and frequency (Delbecke *et al.* 2003).

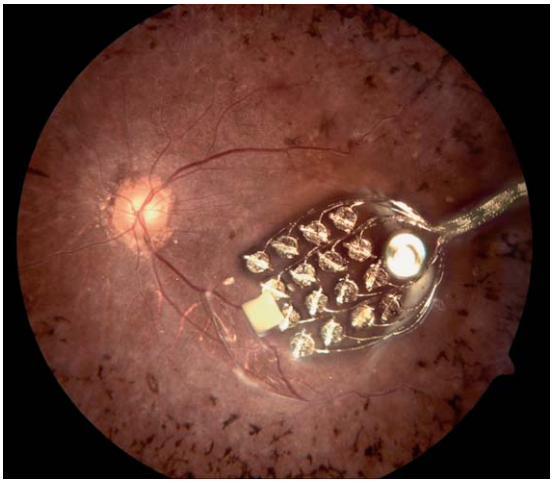

Figure 7 Photograph of a passive epiretinal stimulation array placed on the retina. The array size is about 6 mm × 6 mm and contains 16 stimulation electrodes on a flexible foil. The array is fixed on the retina by a retinal tag placed just to the right of the stimulation electrodes. The stimulation electrodes are connected to electronics outside the eye by a cable that penetrates the sclera (Humayun *et al.* 2003). (Photograph by Jessica Dougall, Copyright 2005, Doheny Eye Institute and Second Sight Medical Products, Inc. All rights reserved, USA.)

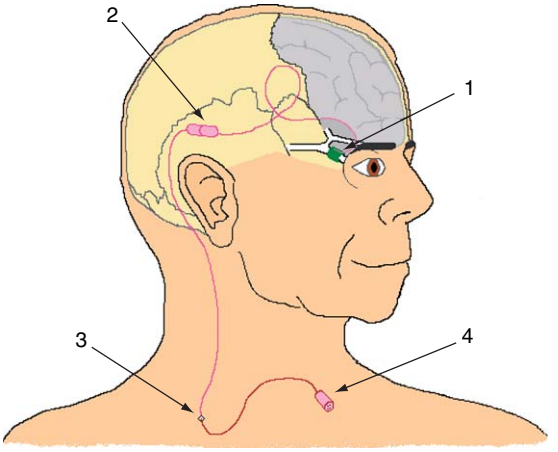

Figure 8 Schematic view of the optic nerve implant system. 1, Cuff electrode; 2, connector; 3, cable; 4, neurostimulator. (Courtesy C Varaart, Université Catholique de Louvain, Belgium.)

Later in 2000, a neurostimulator and an antenna were implanted below the skin and connected to the previously implanted spiral cuff electrode. The X-ray photograph in **Figure 10** shows the different parts of the implanted system (Veraart *et al.* 2003).

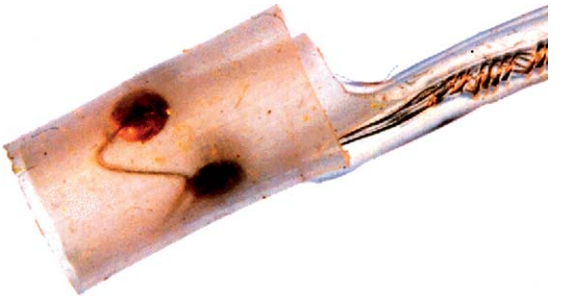

Figure 9 Photograph of the spiral cuff equipped with four electrodes. The electrode diameter is about 3 mm; stimulator dimensions are 25 mm × 30 mm with a 6-mm thickness. (Courtesy C Varaart, Université Catholique de Louvain, Belgium.)

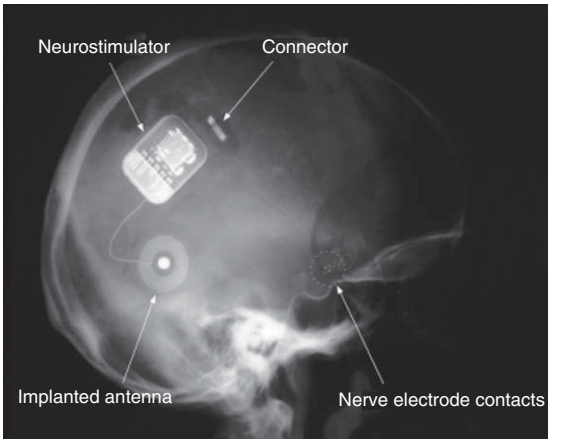

Figure 10 X-ray photograph of the implanted system. (Source: Reprinted from Veraart 2003.)

3.06.3.3 Stimulation of the Visual Cortex

Some patients have lost their vision because the fibers of the optic nerve lost their function. In these cases only a cortical implant can help. Like in epiretinal implants, the hardware components of such a system are a camera that converts light into electrical signals and an implantable interface to the nervous system. In addition, software that converts the image to an appropriate stimulation pattern, thus transforming an image to a retinotropic map, is needed. This information is transmitted to the cortical implant that has stimulation electrodes implanted in the visual cortex (**Figure 11**). By proper stimulation a phosphene pattern is produced. But there is a difference to retinal implants. A square electrode array will elicit a square grid of phosphenes (Dagnellie 2006). Stimulation of the visual cortex will lead to a

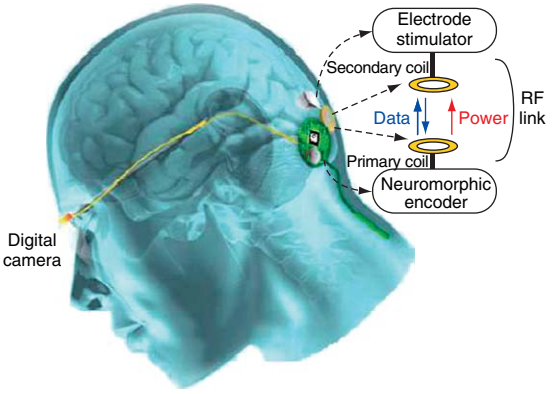

Figure 11 Schema of a cortical neuroprosthesis system. (Source: Reprinted from Piedade *et al.* 2005. © 2005 IEEE.)

phosphene pattern that is likely to be quite irregular. It is necessary to establish crude cortical maps by proper techniques before prosthesis implantation in order to know where to place the electrodes (Dagnellie 2006).

Dobelle *et al.* (1976) performed the implantation of a 64-channel platinum disk electrode array on the surface of the occipital cortex of blind patients. These electrodes were interfaced with a camera consisting of a 100×100 charge-coupled phototransistor array. Random letters were recorded by the camera. According to this information 6 out of the 64 electrodes were stimulated. The patients reported that they were able to recognize characters. However, stimulation on the brain's surface has some drawbacks: to stimulate the target cell in the brain a relatively high voltage is needed and it is not possible to stimulate small groups of cells.

These disadvantages of planar surface electrodes can be overcome by using penetrating electrodes. They can be in direct contact with the target cell. Thus, the voltage needed is drastically reduced (Maynard 2001, Troyk *et al.* 2003). **Figure 12(a)** and **12(b)** shows the configuration Troyk *et al.* (2003) used in their experiments. **Figure 13(a)** and **13(b)** shows two examples of penetrating electrodes developed at the University of Utah (Maynard 2001).

The needle electrodes are about 80 µm in diameter at the base and have a length of 1.5 mm (typically 100 in a 10×10 square grid). They are made from doped silicon. Besides the sharpened tip, the needles are electrically isolated. Each electrode is connected via a bonded, isolated 25-µm wire to a percutaneous connector. Electrode impedances of 100–500 kΩ were measured with a current of

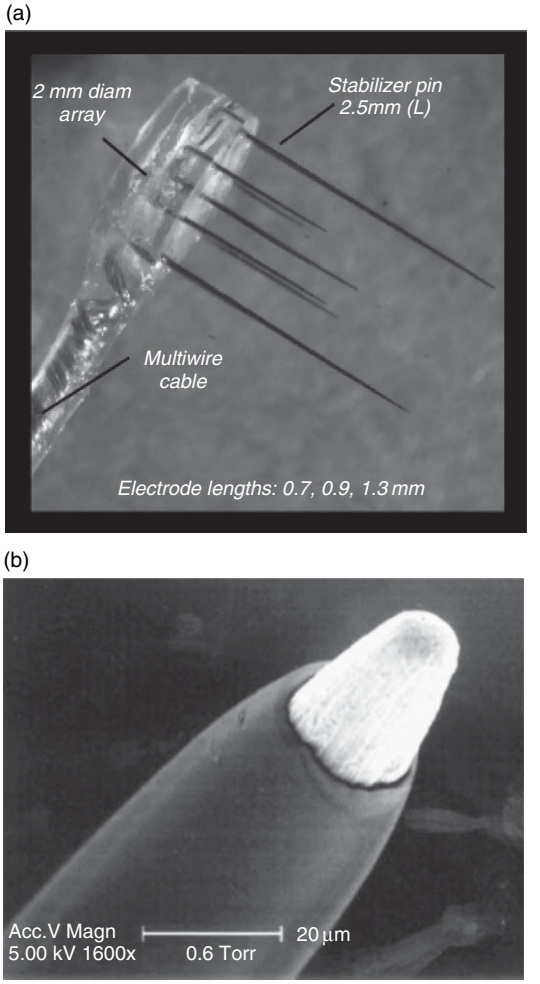

Figure 12 (a) Configuration of HMRI (Hunter Medical Research Institute) arrays used for implantation. The long stabilizer pins help to maintain the position of the array in the cortex (Troyk *et al.* 2003). (b) Scanning electron micrograph of a typical microelectrode tip showing the Parylene insulation and the exposed iridium tip (Troyk *et al.* 2003). (Courtesy P R Troyk, Illinois Institute of Technology, USA, with permission of Blackwell Publishing.)

100 nA at 1 kHz. These electrodes were implanted successfully in trained animals for 100 days.

While the cortical implant has the potential to help a greater number of people than does the retinal implant, it may require a longer investigation period because it involves implanting a device into the brain and because it has not been studied as much as the retinal implant.

3.06.3.4 Biohybrid Retinal Implants

A biohybrid retinal implant combines regenerative medicine with retinal implants. Microelectromechanical

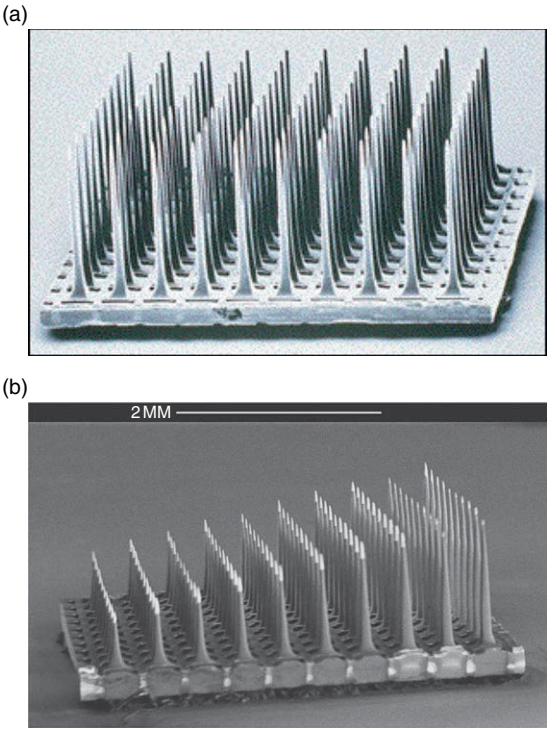

Figure 13 A typical Utah Electrode Array. (b) A modification of the Utah Electrode Array in which the length of the electrodes is uniformly graded. (Source: Maynard E 2001 visual prostheses. *Annu. Rev. Eng.* **3**, 145–68.)

systems (MEMS) is combined with nerve cells that are grown on top of stimulation electrodes. In an epiretinal approach Yagi from Nagoya University cultured nerve cells on top of electrodes (Yagi *et al.* 1999). If nerve cells and Schwann cells are brought together, the lengthening of nerve cells is promoted by factors that are produced in the Schwann cells. An artificial optic nerve can be prepared from Schwann cells and the extracellular matrix. The axons of the nerve cells are guided to the higher visual cortex. They are used as a cable to connect the MEMS electrodes with the visual cortex (**Figure 14**). It is assumed that after a connection of the nerve fibers with nerve cells of the visual cortex is formed, the nerve fibers transmit signals to the visual cortex in response to electrical stimulation of the fibers by a stimulation electrode array (Yagi *et al.* 1999). The hybrid retinal implant requires neither the retinal ganglion cells nor the optic nerve.

For successful electrical stimulation it is necessary that the stimulation electrodes be in close proximity to the nerve cell. This is being studied at Stanford University by using a subretinal approach. The nerve cells are brought in the proximity of the stimulation sites by so-called retinal migration. Retinal cells migrate rapidly (within 48–72 h) into a perforated subretinal implant while preserving their axonal connections to the retina above the implant (Palanker *et al.* 2004a, b, 2005). Within the pores in the implant, stimulating electrodes can be positioned and in this way an intimate proximity between electrodes and target cells is automatically achieved along the whole surface of the implant (**Figure 15**) (Palanker *et al.* 2005).

3.06.4 Technical Challenges

3.06.4.1 Fabrication of Flexible Retinal Implants

During surgery the implant is pushed into the eye through a tiny cut in the cornea. Flexibility and foldability of the implant allow for a smaller cut and

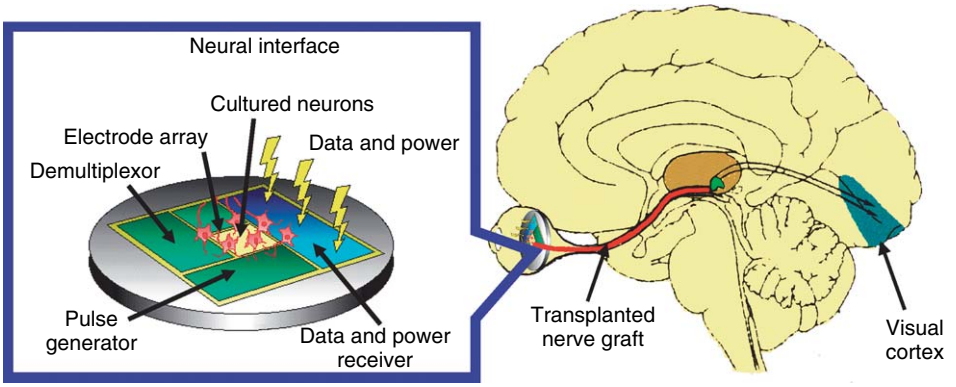

Figure 14 Schematic view of the system proposed by Yagi (Yagi *et al.* 1999). The neural interface consists of a silicon chip with circuitry that communicates with an external system. Neurons are cultured on an electrode array and will grow through a transplanted nerve graft toward the visual cortex. (Source: Yagi T *et al.* 1999 Hybrid retinal implant: Fusion of engineering and neuroscience. *Proc. IEEE Int. Conf. Syst. Man Cybern.* **4**, 382–5.)

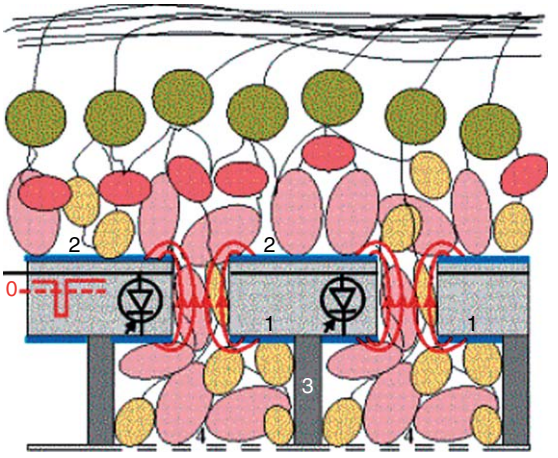

Figure 15 Concept of protruding electrodes on the subretinal array penetrating deep into the retina after migration of the retinal cells into the empty spaces between the pillars. Penetration depth is set according to the length of the pillars, which are insulated at the sides and exposed at the top. (Source: Palanker D *et al*. Design of a high resolution optoelectronic retinal hypothesis. *J. Neural Eng.* **2**, S105–20; reproduced with permission from IOP Publishing Ltd.)

hence less invasive surgery. Because of these requirements, the production of the implant by using a thin polyimide foil and a flexible electroplated coil seems to be the most promising choice (Mokwa 2004).

A typical fabrication process is described in Hungar *et al.* (2005). The polyimide foils are produced using standard and nonstandard wafer-level processes. Silicon wafers (4″) coated with a sacrificial layer are used as substrates for the production process. Polyimide is spin-coated onto the sacrificial layer and structured along the outlines of the implants and around the electrode array in the form of cloverleaves. This structuring is necessary not only to define the separation lines between implants but also to speed up the etching of the sacrificial layer at the end of the production process. In an electroplating step, gold wiring is grown before a second polyimide film is spin-coated and patterned. At this point, the trenches forming the outlines of the implant and the cloverleaves of the electrode array are structured and the openings of the pads and electrodes are etched. A second gold electroplating step is performed to add 26 µm to the height of the electrodes. At this point, the implants could in principle be assembled to fully functional telemetric eye prostheses. However, the electrode material gold has some disadvantages with regard to electrical stimulation of nerve cells. Therefore, a suitable coating material like iridium oxide is added to the electrodes. The coating is done by reactive DC magnetron sputtering from an iridium target in an argon/oxygen plasma (Slavcheva *et al.* 2004). Parylene C is then added from a gas phase to form a biocompatible protective coating. Parylene C has a long history of use in permanent medical implants, and it is an FDA-approved USP class VI polymer and is hence suitable for chronic implantation (Schmidt *et al.* 1988, Yuen *et al.* 1987). On the electrodes, holes are etched into the Parylene C film so that the electrodes can electrically contact the ganglion cells of the retina. A schematic view of the cross section of an electrode and an implant is shown in **Figure 16**.

Finally, the implants are removed from the wafer by etching away the sacrificial layer (Hungar *et al.* 2005). Then the implant is coated with silicone as an additional biocompatible protective layer. As the electrodes have to remain free from silicone, a special mould must be used for this process step. The complete encapsulated implant is shown in **Figure 6**. Biocompatibility and long-term stability of this implant were studied in a simple model (Stieglitz *et al.* 2003). No degradation was found within a period of 1 year.

Figure 17 shows a photograph of a second-generation prototype of the implant shown in **Figure 5** before encapsulation with silicone, with the main components mounted onto a flexible polyimide tape (from left to right): receiver coil, capacitor, diode,

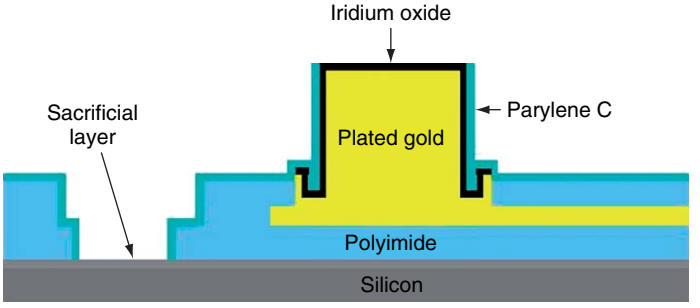

Figure 16 Schematic view of wafer-level cross section of an electrode and an implant.

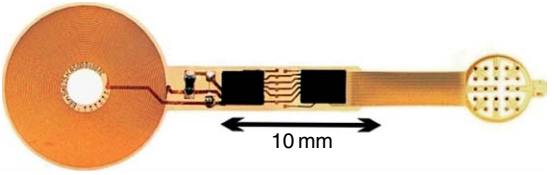

Figure 17 Second-generation prototype of a telemetric eye prosthesis. (Source: Mokwa 2004 MEMS technologies for epiretinal stimulation of the retina. *J. Micromech. Microeng.* **14**, 12–16.)

receiver chip, stimulation chip, microcable, and a 5×5 array of 3D iridium oxide-covered gold electrodes (Mokwa 2004, Wessling *et al.* 2005).

Around the electrodes the polyimide tape is patterned in the shape of cloverleaves, with each carrying four electrodes. This gives the implant additional flexibility, allowing it to be better adapted to the round shape of the retina and hence improving electrical contact between the electrodes and the retina.

3.06.4.2 Stimulation Electrodes

3.06.4.2.1 Requirements for stimulation electrodes

In view of their specific application the implantable electrodes must fulfill several very stringent requirements such as a miniaturized geometry (to match the limited space in the biological units and to ensure a good stimulation selectivity), softness and flexibility (to prevent damage to the surrounding tissue due to mechanical stress), and long-term stability and corrosion resistance (to withstand the corrosive attack of the physiological environment). Biocompatibility is another very important feature of the stimulating electrodes because stimulation must be accomplished without leakage of toxic products that cause damage to the neural cells. However, the most essential precondition for the success of functional electrostimulation (FES) is the availability of highly electroactive electrode materials capable of delivering enough charges across the phase boundary stimulating electrode/stimulated tissue as well as the low impedance of this boundary, especially in the frequency range of 10 Hz to 1 kHz, which is relevant for neural stimulation (Blau *et al.* 1997, Fröhling *et al.* 1996). It is difficult to find a material conforming to all these requirements. Thus, the practical decisions taken are often a compromise.

3.06.4.2.2 Research on stimulation electrodes

In the search for the ideal candidate, microelectrodes of different shapes and sizes have been fabricated, including planar disk electrodes (Agnew *et al.* 1983, Hesse *et al.* 2000, McCreery *et al.* 1990), tethered microwires and intrafascicular electrodes (Googall *et al.* 1993, Naughton and Horch 1996, Silva *et al.* 1998, Yoshida and Horch 1993a, b), cuff electrodes (Duysens and Stein 1978, Meier *et al.* 1986, Schuettler *et al.* 2002, Veraart *et al.* 1998), and various microfabricated 2D and 3D microelectrode arrays (Anderson *et al.* 1989, Rutten 2002, Tanghe *et al.* 1990, Weiland and Anderson 2000). The electroactive metallic materials that have been tested as stimulating electrodes are numerous, the ones most frequently used being Ti, TiN, and different Ti alloys (Blau *et al.* 1997, Haemmerle *et al.* 2002, Walter and Heimann 2000), Au (Haemmerle *et al.* 2002, Hung *et al.* 2002), Pt and some of its alloys such as Pt/W and Pt/Ir (Hesse *et al.* 2000, Lee *et al.* 2002, Yoshida and Horch 1993b), and most recently Ir and IrO_x (Anderson *et al.* 1989, Blau *et al.* 1997, Bolz *et al.* 1995, Fröhling *et al.* 1996, Fröhling *et al.* 1998, Lee *et al.* 2002, Walter and Heimann 2000, Weiland and Anderson 2000).

The performance of a metallic electrode in a physiological fluid environment is mainly determined by the properties of the phase boundary electrode/tissue. This boundary is a complex system exhibiting nonohmic behavior. From a physical point of view it acts as an electrochemical transducer exchanging electrons with ions, the current carriers in the electrode and the electrolyte (body fluid), respectively. As the stimulation of the neuronal action potential depends on the amount of charge transferred across the phase boundary, it is important to select an electrode material that is capable of delivering high charge densities reversibly, i.e., a material that possesses a high charge delivery capacity, Q_{CDC}– a parameter that describes the highest possible charge accumulation at the electrode in a defined environment. The charge delivery must be accomplished safely, which means without occurrence of irreversible processes such as gas evolution due to water electrolysis, major pH changes, metal dissolution, or oxidation of organics that cause damage to the neural cells. A reversible charge injection is possible by two basic mechanisms: capacitive charging and discharging of the electrical double layer formed on the phase boundary and Faradaic redox reactions involving species that remain bound

to the electrode surface. It is ideal from a safety point of view to stimulate only capacitively, and the initial focus has been on the search for capacitive electrodes. An example of such an electrode material is TiN. It has been extensively tested and has shown typical capacitive electrochemical behavior and a very good corrosion resistance in different electrolytes (Haemmerle *et al.* 2002, Janders *et al.* 1997, Walter and Heimann 2000). The capacitive stimulation, although safe, has one essential disadvantage. It seriously limits the transferable charge: generally only 20–30 $\mu C\,cm^{-2}$ are passed during the charging of the electrical double layer of a smooth electrode material (Cambell and Jones 1992). This layer behaves as a parallel plate capacitor and its capacitance is proportional to the electrochemically active surface.

3.06.4.2.3 Enhancement of charge delivery capacity

The miniaturization of the stimulating electrodes enhances the spatial resolution and the selectivity of the stimulation. On the other hand, the smaller the electrode the lower the charge transfer and the higher the impedance of the phase boundary. In order to overcome this contradiction an active area that is as large as possible must be integrated on an electrode of limited size. This can be achieved to some extent by preparing macroporous structures through sintering, etching, electrochemical plating, and plasma-enhanced chemical or physical vapor deposition (Bolz *et al.* 1995, Fröhling *et al.* 1996, Hung *et al.* 2002, Janders *et al.* 1997, Naughton and Horch 1996).

The Faradaic mechanism is an alternative stimulation mechanism that requires the usage of electroactive electrode materials capable of transferring high charges through reversible redox reactions in the safe water window potential range, i.e., between the potentials of H_2 and O_2 evolution. In this case the current flow across the phase boundary is due to changes in the oxidation state of the participating materials. The ability of various noble metals to act through this stimulation mechanism has been studied extensively. For instance, the silver–silver chloride electrode (Ag/AgCl) has been widely used for measuring the action potential. However, it has been found that when in contact with biological tissue, the silver chloride on the surface dissolves and causes inflammations due to its toxicity. That limits its application for stimulation purposes (Moussy and Harrison 1994, Yuen *et al.* 1987). Application of gold, another noble metal known for its biocompatibility, is also restricted (Haemmerle *et al.* 2002, Janders *et al.* 1997) due to the low current densities of its redox reactions in physiological solutions and the narrow potential range in which it shows reversible electrochemical behavior (Slavcheva *et al.* 2002). The elements of the platinum group have received special attention because they have at least two different oxidation numbers and hence higher electrochemical activity. Some of these metals like osmium are toxic, while the charge-delivering capacity of others, for example, palladium, is not high enough (Fröhling 1996). One of the metals that has been used often in FES is platinum (Anderson *et al.* 1989, Hesse *et al.* 2000, Hung *et al.* 1999, Humayun *et al.* 1996, Lee *et al.* 2002, Naughton and Horch 1996, Walter and Heimann 2000, Yoshida and Horch 1993b). It has a stable reversible electrochemical behavior in a comparatively broad potential range (from –0.6 to 1.0 V). Its charge delivery capacity is between 100 and 400 $\mu C\,cm^{-2}$ (Brummer and Turner 1977a, b, Brummer *et al.* 1983, Cambell and Jones 1992) and can be increased by electroplating platinum black on the top of a platinum electrode (Brummer *et al.* 1983, Cambell and Jones 1992, Naughton and Horch 1996). However, these electroplated platinum black films have a flimsy dendritic structure and are mechanically not stable. Hence some amount of charge is always lost due to metal dissolution, especially when used in the long term (Brummer and Turner 1977a, b, Fröhling *et al.* 1996, Hung *et al.* 2002, Janders *et al.* 1997). Some platinum alloys (platinum/tungsten, platinum/iridium) have also been tested as stimulating electrodes. For instance, 70% platinum/30% iridium has been used because of its greater mechanical strength when compared to pure platinum (Robblee *et al.* 1983). Another alloy, 90% platinum/10% iridium, has recently been used in heart pacemakers. A drawback of platinum and its alloys, according to some authors (Gielen and Bergveld 1982), is their unstable impedance in the low-frequency range. Other metals from the platinum group, namely rhodium, ruthenium, and iridium, can take up to four different oxidation states and thus they possess an increased electroactivity. However, it has been demonstrated that in the case of rhodium and ruthenium, the low initial impedance of the phase boundary electrode/electrolyte increases essentially during electrochemical loading and that their long-term stability is not adequate for FES (Fröhling *et al.* 1996). Thus, among all the tested materials, iridium seems to be the most promising

candidate for implantable stimulating electrodes. It is an attractive alternative to platinum mainly because it has four oxidation states (platinum has two) and has shown a superior corrosion resistance. Another characteristic feature of iridium that is beneficial for FES is its ability to form a contact with an aqueous environment, hydrated oxide surface layers, resulting in an increased electrochemically active surface and a higher charge delivery capacity (Robblee *et al.* 1983, Weiland and Anderson 2000). The formation of these oxide layers requires continuous potential cycling between defined lower and upper potential limits specific for the electrolyte medium. The films obtained are known as anodic/activated iridium oxide films (AIROFs). It has been unambiguously proved that AIROFs have a 100-fold higher charge delivery capacity compared to nonactivated pure iridium electrode and a very broad safe potential range (free of gas generation). The problem with these films from the FES point of view arises in connection with their long-term stability (Blau *et al.* 1997).

Another method for producing iridium oxide is by reactive sputtering of iridium in an oxygen atmosphere (Bestaoui *et al.* 1993, Wessling *et al.* 2005). The obtained films, known as sputtered iridium oxide films (SIROFs), have a highly developed fractal surface with a microporous structure and a density of about $10\,g\,cm^{-3}$ (**Figure 18**). SIROFs have unusual electrocatalytic properties and are highly efficient anodes for water electrolysis. They possess a very low overvoltage for oxygen evolution and are stable at high potentials where other catalysts corrode at a significant rate. They also exhibit an outstanding charge delivery capacity (**Table 1**).

Table 1 Charge delivery capacity of different metals

Material	Q_{CDC} ($\mu C\ cm^{-2}$)
Au	490
TiN	687
Pt	4134
Ir	17 078
IrO_x	28 450
IrO_x (after activation)	95 100

3.06.4.3 Appearance of Phosphenes

Phosphenes caused by electrical stimulation may be fuzzy, irregular in shape, varying in size and color, and limited in brightness range and gray-scale resolution; their positions may be scattered relative to an idealized grid (Dagnellie 2006). In retinal prostheses the positional irregularities can be expected to be small, but they can be widely scattered in cortical implants. Therefore, it is very important to determine these properties for each phosphene and to perform inverse image transformation to achieve the closest approximation between the original and the perceived pictures (Dagnellie 2006). For an epiretinal system, Eckmiller and others (Eckmiller 1995, 1997, Eckmiller *et al.* 2005) proposed an adaptive learning retina encoder to perform image preprocessing to optimize stimulus perception by the implant wearer (**Figure 19**). This has to be an interactive and iterative process.

The retina encoder was designed as a neural net with flexible antagonistic receptive field properties (receptive field–adaptive biology–inspired pulse

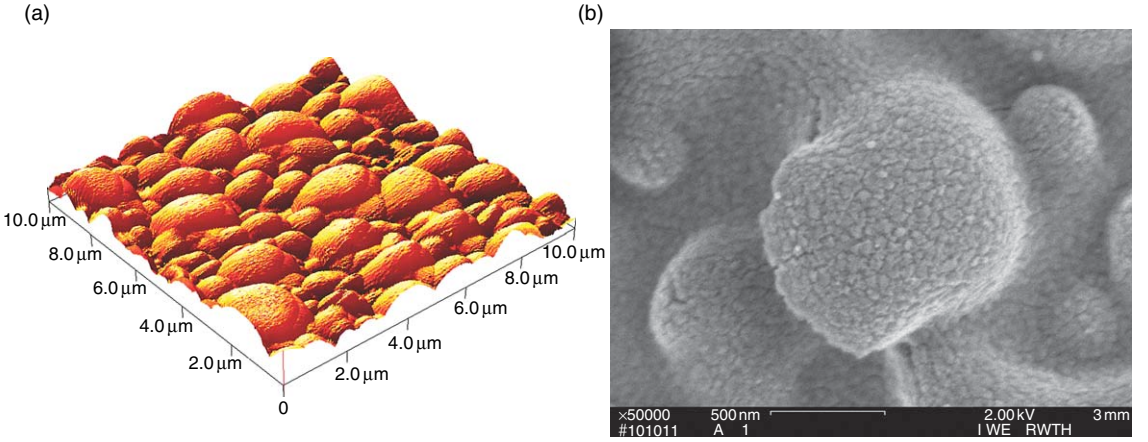

Figure 18 (a) Sputtered iridium oxide film (SIROF) surface after activation (atomic force microscopy). (b) SIROF surface after activation (scanning electron microscopy).

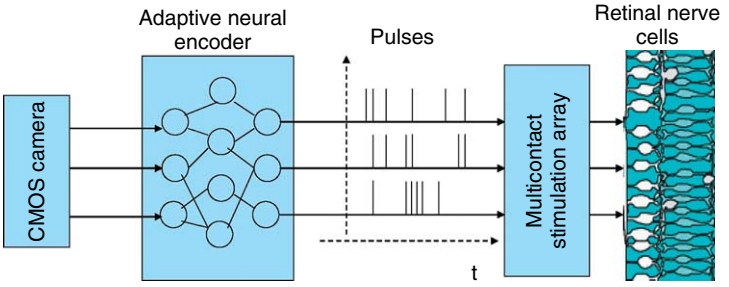

Figure 19 Working scheme of an adaptive encoder.

processing neural network, RF-BPN). The RF-BPN module allows for modification of spatial and/or temporal parameters in order to adjust the RF-BPN to the desired receptive field properties of a given ganglion cell. Specifically, in a learning process each RF-BPN module can be tuned to the receptive field properties of different cell types in the retina with regard to parameters such as RF center and time constants (Eckmiller 1995).

3.06.5 Clinical Studies

3.06.5.1 Verification of Visual Cortex Activation by Epiretinal Stimulation of Animals

In different experimental approaches it could be proven that electrical stimulation of the retina of animals leads to relevant activation of the corresponding areas of the visual cortex. Walter and Heimann (2000) proved the activation by noninvasive recording of evoked potentials after epiretinal electrical stimulation. By recording neuron activity with intracortical electrodes, it could be shown by Schanze, Eckhorn, and coworkers that the stimulation of a distinct area of the retina leads to cortical activation of the corresponding area. The cortex activations after electrical stimulation take place at the same area where the retinal ganglion cells are represented in natural sight (Eger *et al.* 2005, Schanze *et al.* 2002, 2003).

Complete epiretinal systems (compare **Figure 6**) were implanted into mini pigs and cats. Full telemetric functioning could be shown with several systems. **Figure 20** shows a cortical recording from a mini pig after telemetric stimulation of retinal ganglion cells. As expected, the response can be seen in about 25 ms after stimulation (Laube *et al.* 2004a, b).

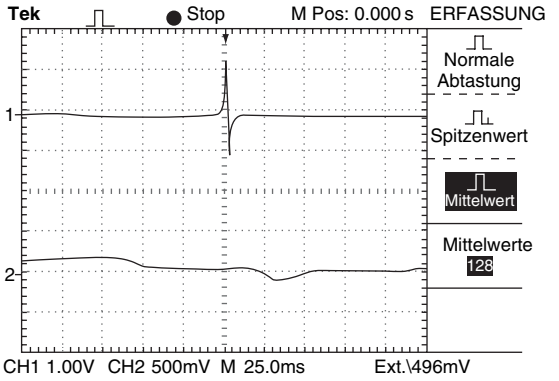

Figure 20 Cortical recording after electrical stimulation of the retinal ganglion cells of a mini pig by a retinal implant (system shown in **Figure 6**); the upper curve shows a stimulation artifact; the lower curve shows the cortical response after electrical stimulation. (Courtesy Laube, Department of Ophthalmology University Essen, Germany.)

In **Figure 21** the area of cortical activity of a cat during electrical stimulation is given. This picture was obtained by the method of optical imaging. The method distinguishes between oxygenized and deoxygenized hemoglobin. Thus, the areas of active and less active metabolism can be distinguished. The areas of increased activation in **Figure 20** correspond to the areas on the retina that had been electrically stimulated (Walter *et al.* 2005).

3.06.5.2 Experiences with Epiretinal Stimulation in Humans

Currently a lot of research activities are going on for developing implantable retina stimulators. The development of epiretinal implants seems to be relatively close to a product. Several working groups have been conducting acute trials on the question whether blind RP patients recognize visual sensations after electrical stimulation. In these trials, electrodes were

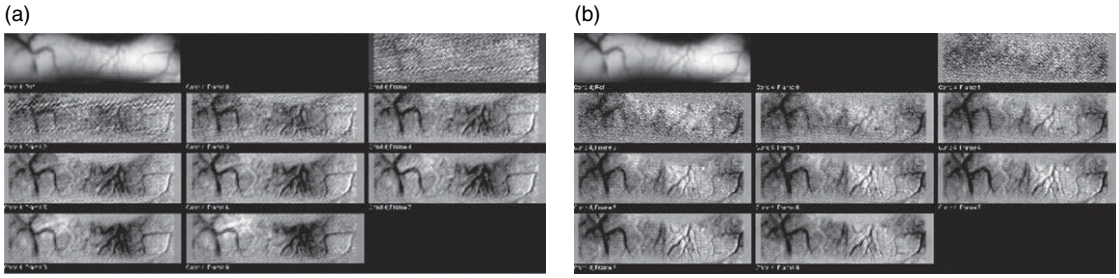

Figure 21 (a) Optical imaging from the visual cortex of a cat during electrical stimulation of the corresponding regions on the retina. The black regions in the right part of the pictures show increased oxygen consumption in areas of the visual cortex that correspond to the stimulated areas of the retina (Walter *et al.* 2005). (b) Control experiment without stimulation pulses (Walter *et al.* 2005). (Courtesy P Walter, Department of Ophthalmology, University Hospital, RWTH Aachen University, Aachen, Germany.)

placed on the retina under the conditions of vitrectomy and the patients were asked whether they had visual sensations. By this the current threshold for stimulation was obtained. The results differ very much partly because of the different experimental conditions for the electrode configuration. Values between several microamperes and milliamperes were reported (Humayun *et al.* 1996, 2003, Rizzo *et al.* 2003a, b).

The US company Second Sight has already implanted a system with 16 stimulation electrodes for chronic application in six patients. The German company IIP Technologies used their system for semichronic studies in two patients (Wickelgren 2006).

3.06.6 Conclusions

Various successful approaches for developing an artificial retina have been presented in this chapter. It is estimated that in a couple of years complete systems will be available for chronic implantation in humans. With respect to the total retina implant system there are still many unanswered and maybe unknown questions with regard to the high complexity of the system. Questions concerning a long-term stable fixation, a long-term stable stimulation, and the minimization of power consumption of the implant have to be answered before chronic implantation in humans.

These examples have shown that MEMS technology is a powerful tool for realizing small and complex electronic implants. This technology will help to increase the functionality of existing systems in a significant way. New applications that nobody thought that they were possible some years ago will be possible. These intelligent implants and prostheses will support the field of home care to a great extent. They will also have a strong impact on clinical research. Implants of the future will have an increased biological part like the biohybrids mentioned earlier.

References

Agnew W F, Yuen T G H, McCreery D B 1983 Morphologic changes after prolonged electrical stimulation of the cat's cortex at defined charge densities. *Exp. Neurol.* **79**, 397–441

Anderson D, Najafi K, Tanghe S J, Evans D A, Levy K L, Hetke J F, Xue X, Zappia J J, Wise K D 1989 Batch-fabricated thin-film electrodes for stimulation of the central auditory system. *IEEE Trans. Biomed. Eng.* **36**, 639–703

Benjamin A, Humayun M S, Hickingbotham S, de Juan E, van den Honert C 1994 Characterization of retinal responses to electrical stimulation of retinal surface of *Rana catesbeiana*. *Invest. Ophthalmol. Vis. Sci.* **35(Suppl.)**, 1832

Bestaoui N, Prouzet E, Deniard P, Brec R 1993 *Thin Solid Films* **235**, 35–42

Blau A, Ziegler C H, Heyer M, Enderst F, Schwitzgebelt G, Matties T, Stieglitz T, Meyer J U, Goepel W 1997 Characterization and optimization of microelectrode arrays for *in vivo* nerve signal recording and stimulation. *Biosens. Bioelectron.* **12**, 883–92

Bolz A, Froehling R, Schmidt K, Schaldach M 1995 Effect of smooth, porous and fractal surface structure on the properties of an interface *J. Mater. Sci. Mater. Med.* **6**, 844–8

Brindley G S, Levin W S 1968 The sensations produced by electrical stimulation of the visual cortex. *J. Physiol. (Lond.)* **196**, 479–93

Brummer S B, Turner M T 1977a Electrochemical considerations for safe electrical stimulation of the nervous system with platinum electrodes. *IEEE Trans. Biomed. Eng.* **BME-24**, 59–63

Brummer S B, Turner M T 1977b Electrical stimulation with Pt electrodes. Estimation of maximum surface redox (theoretical non-gassing) limits. *IEEE Trans. Biomed. Eng.* **BME-24**, 440–3

Brummer S B, Robblee L S, Hambrecher F T 1983 Criteria for selecting electrodes for electrical stimulation: Theoretical and practical considerations. *Ann. N Y Acad. Sci.* **405**, 159–71

Cambell P K, Jones K E 1992 In: Cahn R W, Haasen P, and Kramer E J (eds.) *Materials Science and Technology.* VCH Publishers, New York, Vol. 14, p. 346

Chow A Y 1993 Electrical stimulation of the rabbit retina with subretinal electrodes and high density microphotodiode array implants. *Investig. Ophthalmol. Vis. Sci.* **34**, 835

Dagnellie 2006 Visual prosthetics 2006: Assessment and expectations. *Expert Rev. Med. Dev.* **3(3)**, 315–25

Delbecke J, Oozeer M, Veraart C 2003 Position, size and luminosity of phosphenes generated by direct optic nerve stimulation. *Vis. Res.* **43**, 1091–102

Dobelle W H, Mladejovsky M G, Evans J R, Roberts T S, Girvin J P 1976 'Braille' reading by a blind volunteer by visual cortex stimulation. *Nature* **259**, 111–2

Duysens J, Stein R B 1978 Reflexes induced by nerve stimulation in walking cats with implanted cuff electrodes. *Exp. Brain Res.* **32**, 213–24

Eckmiller R 1995 Towards retina implants for improvement of vision in human with RP – Challenges and first results. *Proc. World Congr. Neural Networks*. INNS Press Hillsdale, NJ, Vol. 1, pp. 228–33

Eckmiller R 1996 Retina implants with adaptive retina encoders. *Proc. RESNA Res. Symp.* **21**, 21–4

Eckmiller R 1997 Learning retina implants with epiretinal contacts. *Ophthal. Res.* **29(5)**, 281–9

Eckmiller R, Neumann D, Baruth O 2005 Tunalble retina encoders for retina implants: Why and how. *J. Neural Eng.* **2**, 91–104

Eger M, Wilms M, Eckhorn R, Schanze T, Hesse L 2005 Retino-cortical information transmission achievable with a retina implant. *Biosystems* **79(1–3)**, 133–42

Fröhling G, Rzany A, Riedmueller J, Bolz A, Schaldach M 1996 Electroactive coating of stimulating electrodes. *J. Mater. Sci. Mater. Med.* **7**, 393–7

Fröhling G, Bolz A, Stroebel J, Rutz M, Lawall P, Schwerdoe H, Schaldach M, Schieffer H 1998 *PACE* **21**, 1239–46

Gielen F L H, Bergveld P 1982 Comparison of electrode impedances of Pt, PtIr (10% Ir) and Ir-AIROF electrodes used in electrophysiological experiments. *Med. Biol. Eng. Comput.* **20**, 77–83

Googall E V, Horch K W, McNaughton T G, Lybbert C M 1993 Analysis of single-unit firing patterns in multi-unit intrafascicular recordings. *Med. Biol. Eng. Comput.* **31**, 257–67

Haemmerle H, Kobuch K, Kohler K, Nisch W, Sachs H, Stelzle M 2002 Biostability of micro-photodiode arrays for subretinal implantation. *Biomaterials* **23**, 797–804

Hesse L, Schanze T, Wilms M, Eger M 2000 Implantation of retina stimulation electrodes and recording of electrical stimulation responses in the visual cortex of the cat. *Graefes Arch. Clin. Exp. Ophthalmol.* **238**, 840–5

Humayun M S, de Juan E, Dagnelie G, Greenberg R, Propst R, Phillips H 1996 Visual perception elicited by electrical stimulation of the retina in blind humans. *Arch. Ophthalmol.* **114**, 40–6

Humayun M S, Prince M, de Juan E Jr., Barron Y, Moskowitz M, Klock I B, Milam A H 1999 Morphometric analysis of the extramacular retina from postmortem eyes with retinitis pigmentosa. *Invest. Ophthalmol. Vis. Sci.* **40(1)**, 143–8

Humayun M, Weiland J D, Fujii G Y, Greenberg R, Williamson R, Little J, Mech B, Cimmarusti V, Van Boemel G, Dagnelie G, de Juan E 2003 Visual perceptions in a blind subject with a chronic microelectronic retinal prosthesis. *Vis. Res.* **43**, 2573–81

Hung A, Zhou D, Greenberg R, Judy J W 2002 Micromachined electrodes for high density neural stimulation systems. *Proc. 2nd Annu. Int. IEEE-EMBS Special Topic Conference on Microtechnologies in Medicine and Biology*. Madison, WI, USA, May 2–4, 2002

Hungar K, Slavcheva E, Spanier G, Mokwa W, Görtz M 2005 Production processes for a flexible retina implant. *Sens. Actuators* **123–4C**, 172–8

Janders M, Egert U, Steltze M, Nish W 1997 *Proc. 18th Annu. Int. Conf. Bridging Disciplines for Biomedicine, IEEE-EMBS*, Amsterdam, The Netherlands, pp. 245–7

Kaufman P L, Alm A 2003 *Adler's Physiology of the Eye*, 10th edn. Mosby, St. Louis, MO

Kuritz T, Lee I, Owens E T, Humayun M, Greenbaum E 2005 Molecular photovoltaics and photoactivation of mammalian cells. *IEEE Trans. Nanobiosci.* **4**, 196–200

Laube T, Brockmann C, Buß R, Lau C, Höck K, Stawski N, Stieglitz T, Richter H A, Schilling H 2004a Optical energy transfer for intraocular microsystems studied in rabbits. *Graefes Arch. Clin. Exp. Ophthalmol.* **242(8)**, 661–7

Laube T, Akguel H, Schanze T, Görtz M, Bolle I, Brockmann C, Bornfeld N 2004b First time successful epiretinal stimulation with active wireless retinal implants in Göttinger minipigs. *Arvo poster no. 4188/B649, Ford Lauderdale*

Lee I S, Wang Ch N, Choi K, Choo M S, Lee J H 2002 Characterization of iridium film as a stimulating neural electrode. *Biomaterials* **23**, 2375–80

Maynard E 2001 Visual prostheses. *Annu. Rev. Biomed. Eng.* **3**, 145–68

McCreery D B, Agnew W F, Yuen T G H, Bullara L 1990 Charge density and charge per phase as cofactors in neural injury induced by electrical stimulation. *IEEE Trans. Biomed. Eng.* **37**, 996–1000

Mokwa W 2004 MEMS technologies for epiretinal stimulation of the retina. *J. Micromech. Microeng.* **14**, 12–16

Moussy F, Harrison J 1994 Prevention of the rapid degradation of subcutaneously implanted Ag/AgCl reference electrodes using polymer coatings. *Anal. Chem.* **66**, 674–9

Naughton T G, Horch K W 1996 Metallized polymer fibers as leadwires and intrafascicular microelectrodes. *J. Neurosci. Meth.* **70**, 103–10

Palanker D, Huie P, Vankov A, Aramant R, Seiler M, Fishman H, Marmor M, Blumenkranz M S 2004a Migration of retinal cells through a perforated membrane: Implications for a high-resolution prosthesis. *Invest. Ophthalmol. Vis. Sci.* **45(9)**, 3266–70

Palanker D, Huie P, Vankov A, Freyvert Y, Fishman H, Marmor M F, Blumenkranz M S 2004b Attracting retinal cells to electrodes for high-resolution stimulation. *Opthal. Technol., SPIE* **5314**, 306–12

Palanker D, Vankov H, Huie P, Baccus S 2005 Design of a high resolution optoelectronic retinal prosthesis. *J. Neural Eng.* **2**, S105–20

Peachey N S, Chow A Y 1999 Subretinal implantation of semiconductor-based photodiodes: Progress and challenges. *J. Rehabil. Res. Dev.* **36**, 371–6

Piedade M, Gerald R, Sousa L A, Tavares G, Tomás P 2005 Visual neuroprosthesis: A non invasive system for stimulating the cortex. *IEEE Trans. Circuits Syst. I Regular Pap.* **52(12)**, 2648–62

Rizzo J F III, Wyatt J, Loewenstein J, Kelly S, Shire D 2003a Methods and perceptual thresholds for short term electrical stimulation of human retina with microelectrode arrays. *Invest. Ophthalmol. Vis. Sci.* **44(12)**, 5355–61

Rizzo J F 3rd, Wyatt J, Loewenstein J, Kelly S, Shire D Perceptual efficacy of electrical stimulation of human retina with a microelectrode array during short term surgical trials. *Invest. Ophthalmol. Vis. Sci.* **44(12)**, 5362–9

Robblee L S, Lefko J L, Brummer S B 1983 An electrode suitable for reversible charge injection in saline solution. *J. Electrochem. Soc.* **130**, 771–3

Rutten W L C 2002 Selective electrical interfaces with the nerve system. *Annu. Rev. Biomed. Eng.* **4**, 407–52

Sachs H G, Gabel V P 2004 Retinal replacement the development of microelectronic retinal prostheses – Experience with subretinal implants and new aspects. *Graefes Arch. Clin. Exp. Ophthalmol.* **242(8)**, 717–23

Santos A, Humayun M S, de Juan E, Greenburg R J, Marsh M J, Klock I B, Milam A H 1997 Preservation of the inner retina in retinitis pigmentosa. A morphometric analysis. *Arch. Ophthalmol.* **115(4)**, 511–5

Schanze T, Wilms M, Eger M, Hesse L, Eckhorn R 2002 Activation zones in cat visual cortex evoked by electrical retina stimulation. *Graefes Arch. Clin. Exp. Ophthalmol.* **240(11)**, 947–54

Schanze T, Greve N, Hesse L 2003 Towards the cortical representation of form and motion stimuli generated by a retina implant. *Graefes Arch. Clin. Exp. Ophthalmol.* **241(8)**, 685–93

Schmidt E M, McIntosh J S, Bak M J 1988 Long-term implants of Parylene C coated microelectrodes. *Med. Biol. Eng. Comput.* **26**, 96–101

Schuettler M, Riso R R, Dalmose A, Stefania D, Stieglitz T 2002 Initial chronic results of flexible sieve electrodes as interface to nerve stumps. *Biomed. Technik* **47**, 696–9

Schwahn H N, Gekeler F, Kohler K, Kobuch K, Sachs H G, Schulmeyer F, Jakob W, Gabel V P, Zrenner E 2001 Studies on the feasibility of a subretinal visual prosthesis: Data from Yucatan micropig and rabbit. *Graefes Arch. Clin. Exp. Ophthalmol.* **239(12)**, 961–7

Schwarz M, Ewe L, Hausschild R, Hosticka B J, Huppertz J, Kolnsberg S, Mokwa W, Trieu H K 2000 Micro implantable visual prostheses. In: *Proc. 1st Annu. Int. IEEE-EMBS Special Top. Conf. Microtechnologies in Medicine and Biology*, Piscataway, NJ, USA, pp. 461–5

Silva T M, Rito J E, Simoes A M P, Ferreira M G S, da Cunha Belo M, Watkins K G 1998 Electrochemical characterization of oxide films formed on Ti–6A1–4V alloy implanted with Ir for bioengineering applications. *Electrochem. Acta* **43**, 203–11

Slavcheva E, Ewe L, Schnakenberg U, Mokwa W 2002 Electrochemical characterization of different biocompatible metallic materials as planar and 3D-electrodes in neural stimulation microarrays. *Proc. 2nd Eur. Conf. Medical and Biological Engineering*, Vienna, Austria, Vol. 3(1), p. 785

Slavcheva E, Ewe L, Schnakenberg U, Mokwa W 2004 Sputtered iridium oxide films as charge injection material for functional electrostimulation. *J. Electrochem. Soc.* **151(7)**, E226–37

Stieglitz T, Haberer W, Kammer S, Schanze T 2003 A simple model to investigate the stability of flexible micromachined retina stimulators. In: *Proc 8th Annu. Int. Conf. International Functional Electrical Stimulation Society*, Maroochydore, Australia, pp. 69–73

Stone J L, Barlow W E, Humayun M S, de Juan E, Jr., Milam A H 1992 Morphometric analysis of macular photoreceptors and ganglion cells in retinas with retinitis pigmentosa. *Arch. Ophthalmol.* **110**, 1634–9

Tanghe S J, Najafi K, Wise K D 1990 A planar IrO multichannel stimulating electrode for use in neural prostheses. *Sens. Actuators* **B1**, 464–7

Troyk P, Bak M, Berg J, Bradley D, Cogan S, Erickson R, Kufta C, McCreery D, Schmidt E, Towle V 2003 A model for intracortical visual prosthesis research. *Artif. Organs* **27(11)**, 1005–15

Veraart C, Raftopoulos C, Mortimer J T, Delbeke J, Pins D, Michaux G, Vanlierde A, Parrini S, Wanet-Defalque M C 1998 Visual sensations produced by optic nerve stimulation using an implanted self-sizing spiral cuff electrode. *Brain Res.* **813(1)**, 181–6

Veraart C, Wanet-Defalque M C, Gerard V, Vanlierde A, Delbeke J 2003 Pattern recognition with the optic nerve visual prosthesis. *Artif. Organs* **27(11)**, 996–1004

Walter P, Heimann K 2000 Evoked cortical potentials after electrical stimulation of the inner retina in rabbits. *Graefes Arch. Clin. Exp. Ophthalmol.* **238(4)**, 315–8

Walter P, Kisvarday Z F, Roessler G F, Alteheld N M, Goertz M, Stieglitz T, Eysel U T 2005 Optical activation via an implanted wireless retinal prosthesis. *Invest. Ophthalmol. Vis. Sci.* **46(5)**, 1780–5

Weiland J D, Anderson D J 2000 Chronic neural stimulation with thin-film, iridium oxide electrodes. *IEEE Trans. Biomed. Eng.* **47**, 911–8

Wessling B, Hungar K, Slavcheva E, Mokwa W, Schnakenberg U 2005 Sputtered iridium oxide as a top layer of stimulating 3D microelectrodes in retina implants. *Biomed. Eng.* **50, Suppl, Vol. 1, Part 1**, 824–3

Wickelgren I 2006 A vision for the blind. *Science* **312**, 1124–6

Wyatt J L, Rizzo J L, Grumet A, Edell D, Jensen R J 1994 Development of a silicon retinal implant: Epiretinal stimulation of retinal ganglion cells in the rabbit. *Invest. Ophthalmol. Vis. Sci.* **35(Suppl.)**, 1380

Yagi T, Ito Y, Kanda H, Tanaka S, Watanabe M, Uchikawa Y 1999 Hybrid retinal implant: Fusion of engineering and neuroscience. *Proc. IEEE Int. Conf. Syst. Man Cybern.* **4**, 382–5

Yoshida K, Horch K 1993a Reduced fatigue in electrically stimulated muscle using dual channel intrafascicular electrodes with interleaved stimulation. *Ann. Biomed. Eng.* **21**, 709–14

Yoshida K, Horch K 1993b Selective stimulation of peripheral nerve fibers using dual intrafascicular electrodes. *IEEE Trans. Biomed Eng.* **40**, 492–4

Yuen G T, Agnew W A, Bullara L A 1987 Tissue response to potential neuroprosthetic materials implanted subdurally. *Biomaterials* **8**, 138–41

Zrenner E 2002 Will retinal implants restore vision? *Science* **295**, 1022–5

Zrenner E, Stett A, Weiss S, Aramant R B, Guenther E, Kohler K, Miliczek K D, Seiler M J, Haemmerle H 1999 Can subretinal microphotodiodes successfully replace degenerated photoreceptors? *Vis. Res.* **39(15)**, 2555

Biography

Wilfried Mokwa received the Dipl.-Phys. degree in Physics from the RWTH Aachen University, Germany, in 1977 and the Dr. rer. nat. degree in 1981 from the same university. From 1981 on he worked at the Department of Experimental Condensed Matter Physics at the RWTH Aachen University on studies of catalytic reactions on gas sensor surfaces. Then he joined the Fraunhofer Institute of Microelectronic Circuits and Systems (IMS) in Duisburg, Germany, in 1985. At the IMS he managed a group working on the monolithic integration of silicon sensors. In 1996 he became a full professor in the Faculty of Electrical Engineering at the RWTH Aachen University where he is director of chair 1 of the Institute of Materials in Electrical Engineering (IWE-1) with special interests in the field of MEMS technologies for medical applications.